# Phononic Metamaterials for Thermal Management: An Atomistic Computational Study

J.-F. Robillard,[1] K. Muralidharan,[1] J. Bucay,[1] P. A. Deymier,[1,*] W. Beck,[2] and D. Barker[2]

[1]*Department of Materials Science and Engineering, University of Arizona, Tucson AZ 85721*

[2]*Department of Physics, University of Arizona, Tucson AZ 85721*

(Received April 12, 2010)

Atomistic computational methods such as molecular dynamics and the Green-Kubo method are employed to shed light on the transport behavior of thermal phonons in models of graphene-based nanophononic crystals comprising periodic arrays of holes. We calculate the phonon lifetime and thermal conductivity as a function of the crystal filling fraction and temperature. The results are interpreted in terms of competition between elastic Bragg scattering and inelastic phonon-phonon scattering. We focus on the effect of the band structure on the phonon lifetime.

PACS numbers: 63.22.Rc, 31.15.xv, 65.80.Ck

## I. INTRODUCTION

Nanofabrication techniques facilitate the structuring of matter in a way that affects the propagation of excitations such as thermal phonons. Indeed, phonons that account for most of the thermal conductivity of a material have a wavelength in the range of 1–100 nm. Thus, a new nanostructured material may be designed in such a way that it has a thermal conductivity that is different from the bulk. This prospect opens up excellent possibilities in at least two research fields, namely, thermal management and thermoelectrics. For example, thermal management is a crucial issue in the field of microelectronics because of the increasing density of devices per unit surface and their unequally distributed emission of heat, which leads to the creation of so-called hot spots. The efficiency of thermoelectric materials can be described by the figure of merit $ZT$, which is proportional to the ratio between the electrical conductivity and the thermal conductivity. Thus, reducing the thermal conductivity of a thermoelectric material could greatly help improve its performance.

Modulating the thermal properties of a material by creating a nanoscale composite material is an approach that has been extensively studied in the case of superlattices [1]. It has been theoretically and experimentally shown that stacks of nanoscale layers impact thermal transport because of the scattering effects of phonons. While superlattices are actually one-dimensional (1D) phononic structures, little is known about the effect of two-dimensional (2D) and three-dimensional (3D) nanophononic structures on thermal conductivity. Most studies on 2D and 3D phononic crystals (PCs) have focused on macroscopic elastic systems. Early experimental and theoretical studies of bulk elastic PCs (i.e., crystals of infinite extent along all spatial directions) have shown that the bandwidth of the

 © 2011 THE PHYSICAL SOCIETY OF THE REPUBLIC OF CHINA

forbidden band of these structures depends strongly on the contrast between the physical characteristics of the inclusions and the matrix, as well as the geometry of the array of inclusions, the inclusion shape, and the filling factor of inclusions [2–4]. In particular, large contrast between the elastic parameters and the mass density of the inclusions and of the matrix is necessary for the existence of band gaps in the acoustic band structure of these composite materials [5]. Theoretical studies had shown the existence of omnidirectional (absolute) band gaps [3, 6, 7] before their experimental observation in various 2D PCs [8–12]. Recent investigations of perfect and defect-containing PCs have revealed a rich range of behaviors, such as those associated with (a) linear and point defects [13], (b) wave bending and splitting [14], and (c) transmission through perfect [15, 16] or defect-containing [16] waveguides. Various authors have theoretically studied the existence of surface acoustic waves (SAWs) localized at the free surface of a semi-infinite 2D PC [17–20], and Lamb modes in PC plates [21, 22]. Other theoretical studies have focused on truncated crystals [23] and wave guiding in passive [24] and piezoelectric PC plates [25]. The experimental preparation of PCs and experimental fabrication of devices followed their theoretical discovery [26–28]. Theoretical and experimental studies of elastic wave propagation in perfect 3D PCs have also revealed the existence of full band gaps [29–36] and of localized modes in defect-containing structures [37, 38]. Negative refraction of acoustic waves has also been shown in PCs [39–43]. In such PCs, the elastic wave band structure exhibits a pass band with a negative group velocity. Focusing of sound using lenses comprising negatively refracting 2D and 3D PCs [44–46]. A variety of other unusual refractive properties of PCs include direction-dependent refraction that can range from positive to negative refraction [47]. The large body of knowledge accumulated on the behavior of elastic macroscopic-scale PCs suggests that it may be possible to downscale the PCs to a size on the order of nanometers; such downscaling can influence the propagation characteristics of phonons with frequencies exceeding the THz range [48]. Recently, Gillet *et al.* [49] have reported simulations of atomic-level phononic structures comprising 3D lattices of Ge quantum dots in a Si matrix. They have shown that the thermal conductivity decreases by several orders of magnitude because of the periodic structure of the system.

In this study, we consider the nanophononic structure of a 2D matrix material that comprises a periodic array of holes with a lattice constant of the order of nanometers. We focus on graphene, or single-layer graphite, which has been the subject of intense theoretical and experimental studies since its first synthesis a few years ago. Indeed, owing to its 2D atomic structure and the properties of the $sp^2$ C-C bonds, graphene exhibits unique electronic properties. However, graphene also has a high thermal conductivity, which makes it a promising material for thermal management of semiconductor electronic devices. In this study, we consider simulations on the atomic scale using molecular dynamics (MD) in conjunction with the Green-Kubo method to determine the phonon dispersion curves as well as the thermal conductivity. Our results show that the thermal conductivity of single-layer graphene can be modulated by transforming its structure to a nanophononic crystal structure. In particular, we show that the filling fraction of the phononic structure plays a major role in controlling the thermal conductivity.

## II. THEORY

In this section we focus on the underlying physics of heat transport in solids. We describe only the phonon-assisted heat conduction and attempt to stress the relevant quantities for a better understanding of the methods and results. Thermal conductivity is defined at the macroscopic scale by the Fourier law:

$$q = -k\nabla T \tag{1}$$

where $\boldsymbol{q}$ is the heat flux, $\nabla T$ is the spatial gradient of temperature, and $\boldsymbol{k}$ is the thermal conductivity tensor. At the microscopic scale the transport of heat is described by the propagation of the phonons. The phonons propagate under the effect of the temperature gradient, which results in a local non-equilibrium distribution. This motion is described by the Boltzmann transport equation (BTE):

$$V_g \cdot \nabla T \frac{\partial f_t}{\partial T} = \left(\frac{\partial f_t}{\partial t}\right)_c \tag{2}$$

where $\boldsymbol{V_g}$ is the phonon group velocity, $f_t$ is the phonon distribution function, and the right-hand side term is the partial derivative of $f_t$. This latter term describes the evolution of the distribution under the influence of the various collision processes. The non-equilibrium distribution $f_t$ can be written as $f_t = f + f'$, where $f$ is the equilibrium distribution and $f'$ is the fluctuating part of the distribution function. While the left-hand side of Eq. (2) describes the motion of non-interacting particles, the right-hand side couples the different phonon modes to one another and with their environment. The collisions of the phonon modes play a significant role in the heat transfer and are usually complex to describe. The relaxation-time approximation is commonly used to make the problem easier to solve. Under that approximation it is assumed that the collision term of Eq. (2) can be written as:

$$\left(\frac{\partial f_t}{\partial t}\right)_c = -\frac{f'}{\tau} \tag{3}$$

where $\tau$ is the phonon lifetime. A more detailed discussion of the BTE and the relaxation-time assumption can be found in [50]. With this assumption we assume that this lifetime includes the contributions of various collision processes, each having a characteristic decay time. This is described by Matthiessen's rule in Eq. (4), where $\tau_{ph}, \tau_e, \tau_d$, and $\tau_b$ are the phonon decay times due to collisions with other phonons, electrons, intrinsic defects, and crystal boundaries, respectively.

$$\frac{1}{\tau} = \frac{1}{\tau_{ph}} + \frac{1}{\tau_e} + \frac{1}{\tau_d} + \frac{1}{\tau_b} \tag{4}$$

In this paper we do not treat electron-phonon scattering. To simplify the problem we can consider an infinite and intrinsic-defect free crystal, so that the contributions of boundary and defects are irrelevant. However, in addition to phonon-phonon scattering, the PCs we

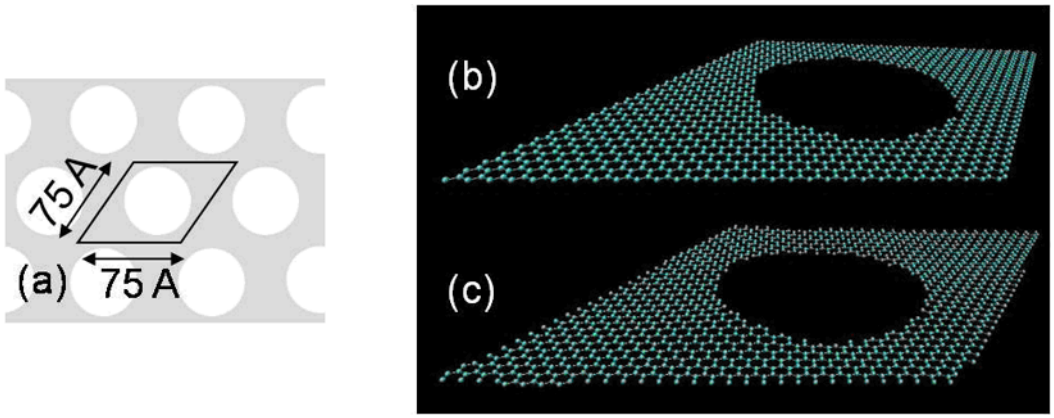


FIG. 1: (a) Scheme of the 2D phononic crystals comprising a triangular lattice of holes on a graphene surface. The lattice constant of 75 Å corresponds to 30 unit cells of the graphene crystal. (b) Atomic structure of the simulation cell before any simulation for a filling fraction of 25%. (c) The same simulation cell after minimization of the energy via the molecular dynamics algorithm. Redistribution of the energy due to the hole boundary results in a slight bending of the graphene surface. Geometry optimization was carried out at constant pressure (P = 0 Pa) conditions.

study here will include phonon-hole inclusions scattering, more specifically scattering by the periodic arrangement of these inclusions. In our case, the lifetime of the phonons is controlled by the competition between inelastic collisions with other phonons and elastic Bragg scattering via the periodic structure of the nanophononic crystal. Using Eqs. (1) to (3) the thermal conductivity tensor can be written as:

$$k = \sum_{\kappa} \sum_{\nu} c_{ph} V_g V_g \tau \tag{5}$$

where $c_{ph}$ is the phonon volumetric specific heat. The summation is over every phonon branch $\boldsymbol{\nu}$ with $\boldsymbol{\kappa}$ vectors in the first Brillouin zone of the lattice. For a given temperature, the main factors that can lead to a modulation of the thermal conductivity are the group velocity and the phonon lifetimes. PCs, by design, can be used to modify phonon band structures, thus providing a means of controlling the group velocity. In an indirect way, modifications of the band structure may lead to constraints on possible phonon-phonon collisions, resulting in changes in the phonon lifetimes.

## III. MODEL AND METHODS

We study a series of PCs comprising a single graphene sheet with hole inclusions. The holes are arranged on a triangular lattice with a fixed lattice parameter $a_{pc}$ = 75 Å(Fig. 1(a)). Thus, the simulation cell consists of 30 × 30 graphene unit cells. The radius of the hole is a variable. We use a MD method to simulate the graphene-based PCs. Prior to forming the PCs by creating holes, the perfect graphene simulation cell contains 1800

atoms. The simulation cell is therefore a 75 Å × 75 Å rhombus. Periodic arrays of holes are formed by removing atoms.

Figure 1(b) shows an example of the simulation cell with a hole before any simulation. The phononic structures are characterized by their filling fraction, $p$, defined as the ratio of the number of atoms removed $N_R$ to the initial number of atoms $N$. This atomic filling fraction is equivalent to the surface area fraction to within a few percent. In every simulation, 2D periodic boundary conditions (PBC) are applied, while there are no restrictions on atomic motion in the third dimension. PBC may constrain some of the long-wavelength phonons in the perfect graphene simulation cell. However, PBC are fully compatible with the phonon band structure of the periodic phononic structures. To model the graphene-based PCs, we employ the Tersoff interatomic potential [51], which is a three-body potential function that explicitly includes an angular contribution to the energy. This potential is widely used at present in various applications for covalently bonded materials such as carbon. Parameters used in this study can be found in the literature [51]. The Tersoff potential includes the anharmonic contributions and is therefore suitable to describe inelastic phonon-phonon processes. The MD simulation consists of integrating the equations of motion of each individual atom over time with an integration step of $10^{-15}$ s. The thermal conductivity of the graphene-based PCs is calculated using the Green-Kubo method [52]. The thermal conductivity is related to the time of relaxation of fluctuations of the heat current by:

$$k = \frac{1}{k_B V T^2} \int_0^\infty \frac{\langle S(t) \cdot S(0) \rangle}{3} dt \tag{6}$$

where $< S(t) \cdot S(0) >$ is the heat-current autocorrelation function, $k_B$ is the Boltzmann constant, and $V$ is the volume of the simulation cell. The heat current $\boldsymbol{S}$ is defined as:

$$S = \sum_i E_i V_i + \frac{1}{2} \sum_{i,j} (F_{ij} \cdot V_i) r_{ij} + \frac{1}{6} \sum_{i,j,k} (F_{ijk} \cdot V_i)(r_{ij} + r_{ik}) \tag{7}$$

where $E_i$ is the total energy of the atom $i$, $\boldsymbol{V}_i$ is its velocity, $\boldsymbol{F}_{ij}$ is the two-body force between atoms $i$ and $j$, $\boldsymbol{r}_{ij}$ is their relative position vector, and $\boldsymbol{F}_{ijk}$ is the three-body force between atoms $i$, $j$, and $k$. The first term in Eq. (7) corresponds to a convective current, and the second and third terms account for heat conduction due to two- and three-body interactions. In this study we focus on the thermal conduction and limit the calculation of the heat current to the last two terms.

The Green-Kubo MD method is an equilibrium approach and requires the system to be simulated in the microcanonical ensemble (constant energy). The simulations reported here are conducted in the same way, namely, equilibration of the simulation cell for one million integration time steps under isothermal conditions using a momentum rescaling method. The system is then simulated under constant energy conditions for another three million time steps. In this case, the temperature fluctuates about the temperature set in the isothermal part of the simulation. Heat-current autocorrelation functions are calculated

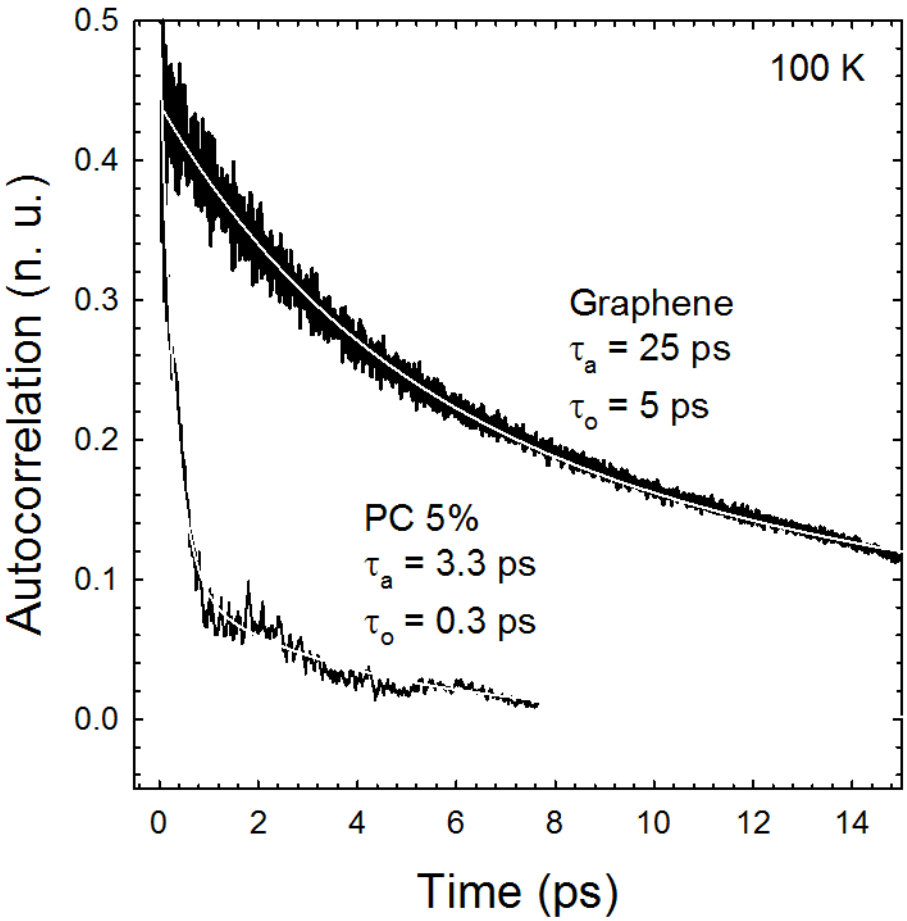


FIG. 2: Typical computed heat-current correlation functions for graphene and for the 5% filling fraction nanophononic crystal at 100 K (solid black lines). The functions exhibit a two time-scale decay reproduced by the sum of two exponential curves (dashed white lines). The two time constants extracted from this curve fitting are a good estimate of the mean lifetimes of the acoustic and optical phonons, $\tau_a$ and $\tau_o$ respectively. The lifetimes in the nanophononic system are observed to be shorter than in graphene; this difference leads to a decrease in the thermal conductivity of the phononic crystals.

during only the last two million steps of the constant energy part of the simulation. All dynamical simulations are conducted at constant volume.

Because the calculated heat-current autocorrelation functions exhibit long time oscillations that may impact the accuracy of their numerical integration, we fit them to exponentially decaying functions. Furthermore, as shown in Fig. 2, these autocorrelation functions appear to exhibit two-stage decay and are, following [52], fitted to the sum of two

exponential functions of the form:

$$\frac{\langle S(t) \cdot S(0) \rangle}{3} = A_a \exp(-t/\tau_a) + A_o \exp(-t/\tau_o) \tag{8}$$

Since the unit cell of the graphene-based structures is diatomic, the short decay time (here $\tau_o$) has been interpreted as resulting from optical phonons, and the long decay time (here $\tau_a$) has been associated with acoustic phonons following [53]. In some cases (higher filling fractions or temperature), a single exponential fit is more suitable. In that case we do not attribute the corresponding lifetime to a given type of phonon mode. However, the fit still provides an estimate of the mean lifetime of phonons. The thermal conductivity is then calculated in the form:

$$k = k_a + k_o = \frac{1}{k_B V T^2} \left( A_a \tau_a + A_o \tau_o \right) \tag{9}$$

where $k_a$ and $k_o$ are the contributions to the thermal conductivity of acoustic and optical phonons, respectively.

In addition to the Green-Kubo MD numerical calculation of thermal conductivity, we calculate the phonon band structure of the graphene-based PCs using the GULP software package under the quasi-harmonic approximation [54]. The atomic configurations used for these calculations are fully relaxed using a steepest-descent method. In spite of this relaxation, for a few filling fractions ($> 25\%$), the band structures exhibit a couple of shallow bands with negative eigenvalues (frequencies). The geometry, and thus the stability, of the simulation cell changes for every filling fraction, and these negative frequencies may result from soft modes associated with atoms on the surface of the hollow inclusions. In Fig. 1(c), we plot the relaxed 25% filling fraction simulation cell. The graphene sheet is slightly warped as a result of the relaxation process.

## IV. RESULTS AND DISCUSSION

The thermal conductivity of the system under study is examined as a function of the filling fraction of holes at two different temperatures (100 K and 300 K). We report in Fig. 3(a) the thermal conductivity $k$ of the graphene-based PC as well as the contribution of the optical and acoustic phonons to the thermal conductivity as functions of the filling fraction of holes at a temperature of 100 K.

We also plot, in the inset of Fig. 3(a), the thermal conductivity as a function of filling fraction calculated based on Vegard's law (parallel model) where $k = p \times k_{\text{graphene}}$, and a Maxwell model where $k = k_{\text{graphene}}(1-p)/(1+p)$. The decrease by nearly one order of magnitude in the thermal conductivity as the filling fraction increases to only 2.5% cannot be explained by these macroscopic mixing laws. Figure 3(b) shows that the lifetime of acoustic and optical phonons also decreases drastically as the filling fraction changes from 0 to 5%. The sharp decrease in lifetime of the acoustic phonons amounts to approximately one order of magnitude and is comparable to that of the thermal conductivity, indicating

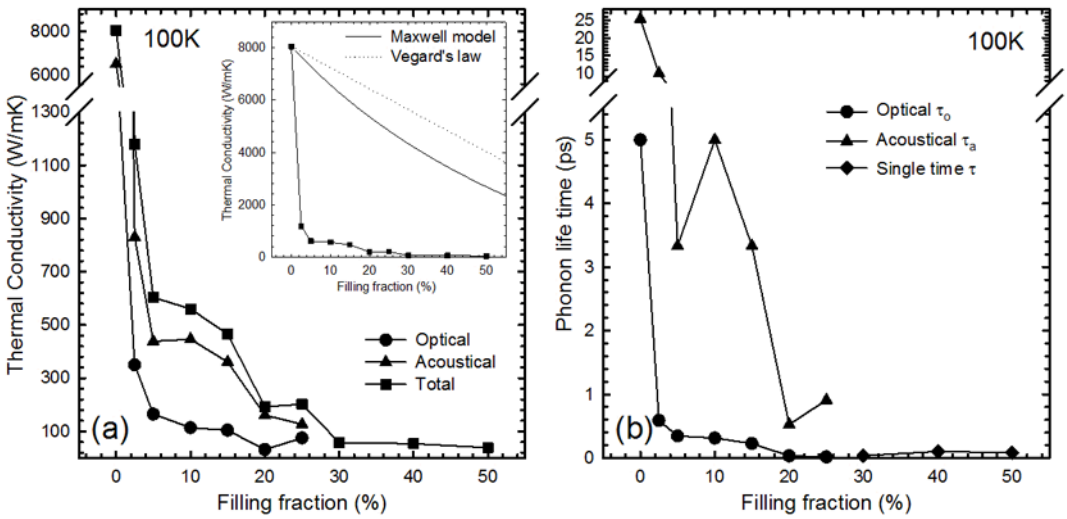


FIG. 3: (a) Thermal conductivity deduced from the Green-Kubo method as a function of the filling fraction at 100 K (squares). For filling fractions below 30%, the contribution of the optical (circles) and acoustic (triangles) phonons are distinguished. Data are compared to a parallel (dotted line) and Maxwell (solid line) mixing model. The drop of thermal conductivity (85%) observed with a fraction of holes as low as 2.5% cannot be explained by these continuous models. (b) Mean acoustic and optical phonon lifetimes as a function of the filling fraction at 100 K. These lifetimes are estimated from the fit of the heat-current correlation functions. The phononic structure is responsible for the drop in the lifetime of acoustic phonons, which are the main contributors to the heat conduction. Error bars on calculated lifetime and thermal conductivity due to the exponential fit of the heat-current autocorrelation functions are the size of the data points.

that the effect of filling fraction on thermal conductivity is due to scattering of the acoustic phonons by the periodic array of inclusions. Phonons with any wave vector originating from the center of the Brillouin zone of the system and ending up on the zone boundary will satisfy the Bragg condition. The insertion of a periodic array of hole inclusions in a graphene sheet reduces the size of the Brillouin zone compared to the perfect graphene sheet. The folding of the bands inside the reduced Brillouin zone of the PC leads to a significant increase in the number of phonon modes that will satisfy the Bragg condition. This can be seen in Fig. 4, where the band structure of the model graphene sheet is contrasted with that of the 5% filling fraction graphene-based phononic structure.

The increase in phonon modes that undergo Bragg scattering is believed to be the primary cause of the reduction in phonon lifetime and thermal conductivity at low filling fraction. This result also indicates that at the temperature of 100 K Bragg scattering by the periodic array of hole inclusions at low filling fraction dominates phonon-phonon scattering. In this case, the lifetime associated with Bragg scattering is shorter than that associated with phonon-phonon scattering. The lifetime due to inelastic scattering is of the order of 25 ps (lifetime for the perfect graphene model). Using Eq. (4) for phonon-phonon and phonon-

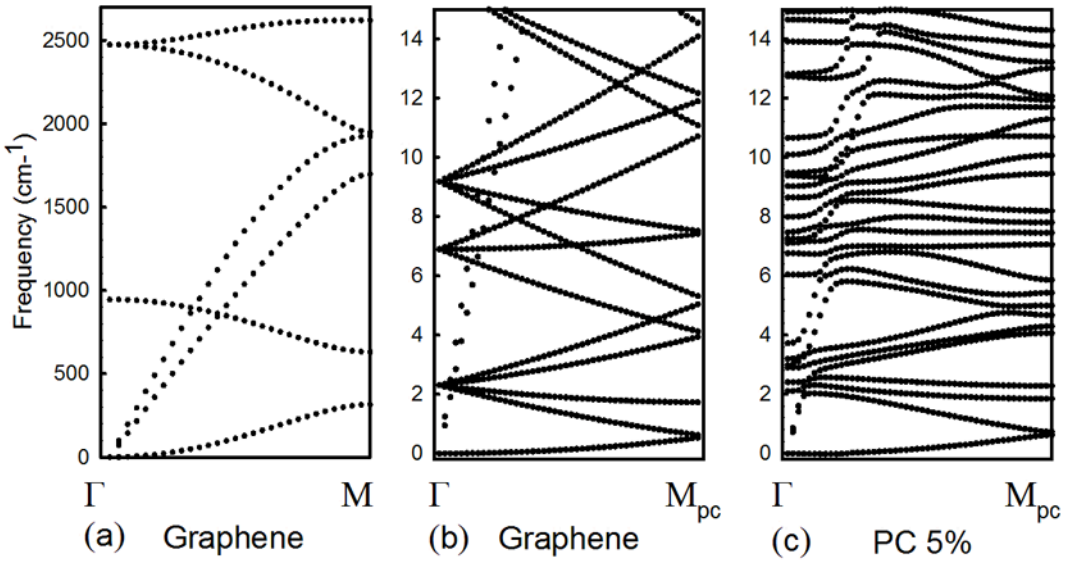


FIG. 4: (a) Phonon band structure of graphene obtained with the Tersoff [51] potential. The results are accurate in the low-frequency part of the spectra. The M point in the pure graphene case is at $\pi/a$, where $a$ is the interatomic distance. (b) Low-frequency part of the band structure of graphene plotted in the $\Gamma M_{pc}$ direction of the graphene-based phononic crystals. The $M_{pc}$ point for the phononic crystals is at $\pi/a_{pc}$. (c) Band structure in the ΓM direction for the graphene-based phononic crystal with a filling fraction of 5%.

defect (hole) scattering, we estimate the lifetime for Bragg scattering at the filling fraction of 5% to be approximately 3.8 ps. There appear to be two regimes in the dependency of acoustic phonon lifetime ($\tau_a$) with filling fraction; for filling fractions between 2.5% and 15%, $\tau_a$ remains of the order of a few ps. Beyond 15%, the autocorrelation functions exhibit much lower decay times, and in fact beyond 25%, a single decay time is sufficient to describe the autocorrelation function. This lifetime is one order of magnitude lower (0.2 ps) compared to the results of lower filling fraction. This drop cannot be solely explained by the effect of the filling fraction on Bragg scattering. The number of modes at the zone boundary scales as $N_z = 3N(1-p)$. Assuming that the lifetime due to Bragg scattering is inversely proportional to $N_z$, no significant changes are expected prior to the limit of a filling fraction of 68%. Assuming an overall lifetime of approximately 0.2 ps for filling fractions in excess of 30% and a lifetime for elastic scattering of 3.8 ps, using Eq. (4) we estimate a lifetime for inelastic scattering of approximately 0.21 ps. This estimate suggests that this change of regime is due to a modification in inelastic scattering caused by a change in band structure with filling fraction.

A comparison of Fig. 3 with Fig. 5, which depicts the variation in thermal conductivity at 300 K, shows the effect of temperature on thermal conductivity and phonon lifetimes.

By increasing temperature, the thermal conductivity and the corresponding lifetimes of optical and acoustic phonons of pure graphene have been significantly reduced as com-

pared to 100 K. This is in contrast to the PC systems where the effect of temperature is less pronounced. The large number of phonons at 300 K leads to an increase in phonon-phonon scattering and an overall reduction in lifetime, implying that this mechanism becomes an equally limiting process along with phonon-hole Bragg scattering in determining thermal conductivity. For the PCs beyond 15% filling fraction, a significant drop in the lifetime of phonons (exceeding a factor of 4) is still noted. This observation attests to the existence of Bragg scattering even at 300 K, where inelastic phonon-phonon collisions start to compete with the elastic Bragg scattering.

Similar to that at 100 K, there is a significant drop in thermal conductivity between pure graphene and the PC at 2.5% filling fraction. However, the drop is reduced from 85% (at 100 K) to 64% (at 300 K). It is worth noting that these drops in thermal conductivity for our 2D system are comparable to those observed for a 3D SiGe PC [49]. Since at 300 K, the phonon lifetimes of pure graphene as well as low filling fraction PCs are comparable (a few ps), the reduction arises only from the respective contributions of the pre-factors $A_a$ and $A_o$ (see Eq. 9). The difference between the calculated thermal conductivity as a function of filling fraction and the Vegard and Maxwell models continues to indicate that significant scattering by the periodic holes occurs.

To shed additional light on the competition between elastic and inelastic scattering in the PCs, the following shows the relationship between the lifetime $\tau$ of phonons and the third-order derivative of the interatomic potential as proposed by [55]:

$$\begin{aligned}
\frac{1}{2\tau(\kappa,\nu)} &= \frac{\pi\hbar}{16N}\sum_{\kappa',\nu'}^{N,6}\sum_{\kappa'',\nu''}^{N,6}\Phi\begin{pmatrix}\kappa & \kappa' & \kappa''\\ \nu & \nu' & \nu''\end{pmatrix}\\
&\cdot\left\{\left[f\begin{pmatrix}\kappa'\\ \nu'\end{pmatrix}+f\begin{pmatrix}\kappa''\\ \nu''\end{pmatrix}+1\right]\left[\delta\left(\begin{pmatrix}\kappa\\ \nu\end{pmatrix}-\omega\begin{pmatrix}\kappa'\\ \nu'\end{pmatrix}-\omega\begin{pmatrix}\kappa''\\ \nu''\end{pmatrix}\right)\right]\right.\\
&+\left[f\begin{pmatrix}\kappa'\\ \nu'\end{pmatrix}-f\begin{pmatrix}\kappa''\\ \nu''\end{pmatrix}\right]\\
&\left.\cdot\left[\delta\left(\begin{pmatrix}\kappa\\ \nu\end{pmatrix}-\omega\begin{pmatrix}\kappa'\\ \nu'\end{pmatrix}-\omega\begin{pmatrix}\kappa''\\ \nu''\end{pmatrix}\right)-\delta\left(\begin{pmatrix}\kappa\\ \nu\end{pmatrix}-\omega\begin{pmatrix}\kappa'\\ \nu'\end{pmatrix}+\omega\begin{pmatrix}\kappa''\\ \nu''\end{pmatrix}\right)\right]\right\},
\end{aligned}\tag{10}$$

where $\Phi$ contains the third-order derivative of the interatomic potential, $(\boldsymbol{\kappa},\boldsymbol{\nu})$ represents a phononic mode of wave vector $\boldsymbol{\kappa}$ in the $\boldsymbol{\nu}^{\text{th}}$ branch in the band structure, $f$ is the equilibrium distribution as defined in section II, $\delta$ is the Dirac function, and $N$ is the number of atoms of the material.

This equation is limited to the effect of three phonon processes on the lifetime. It relates the first non-linear component of the potential to the possibility that a phonon will decay into two different phonons or that two phonons will combine to generate a third one. The delta functions ensure the conservation rules for energy ($\omega$) and momentum ($\boldsymbol{\kappa}$). This equation enables us to discuss qualitatively the effect of several factors, namely, temperature, filling fraction, and band structure. Thermal effects enter Eq. (10) via the equilibrium distribution $f$. As temperature increases, the phonon occupation number of high-energy

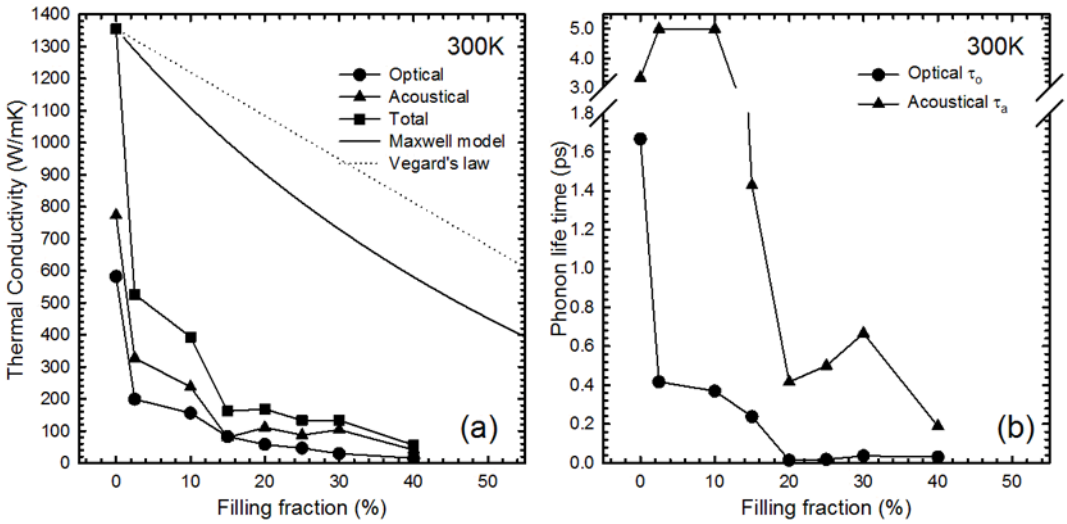


FIG. 5: (a) Thermal conductivity deduced from the Green-Kubo method as a function of the filling fraction at 300 K (squares). The contribution of the optical (circles) and acoustic (triangles) phonons are distinguished. Data are compared to a parallel (dotted line) and Maxwell (solid line) mixing model. (b) Mean acoustic and optical phonons lifetimes as a function of the filling fraction at 300 K. Lifetimes are estimated from the fit of the heat-current correlation functions. Error bars on calculated lifetime and thermal conductivity due to the exponential fit of the heat-current autocorrelation functions are the size of the data points.

bands increases. As a consequence, there will be significantly more phonon decay processes, thus reducing lifetime. This is consistent with our MD results when temperature is increased from 100 to 300 K, independently of the filling fraction.

The filling fraction may impact directly the lifetime via the denominator in Eq. (10). It may also affect the lifetime indirectly via the number of possible three phonon processes accounted for in the summation. A third indirect effect is through the band structure itself. The bands $\nu$ and associated vector $\boldsymbol{\kappa}$ do depend on filling fraction, as shown in Fig. 3. The three phonon processes may then be frustrated or enhanced by changing the band structure $\omega(\boldsymbol{\kappa})$, as these processes must satisfy the conservation laws:

$$\begin{aligned} \omega(\kappa) &= \omega(\kappa') + \omega(\kappa'') \\ \vec{\kappa} &= \vec{\kappa}' + \vec{\kappa}'' \end{aligned} \tag{11}$$

At present, it is not straightforward to resolve these effects using the MD method. Nevertheless, our results as given in Fig. 3(b) suggest such an effect.

## V. CONCLUSIONS

We performed MD simulations of and band structure calculations for graphene-based nanophononic crystals comprising periodic arrays of hole inclusions. Calculations of the heat-current autocorrelation using the Green-Kubo equilibrium method enabled us to estimate the lifetimes of acoustic and optical phonons as well as the thermal conductivity as functions of the PC's filling fraction and the temperature. We have shown that Bragg scattering of thermal phonons leads to dramatic changes in the phonon lifetimes for filling fractions as low as 2.5% over a significant temperature range. This change in lifetimes is followed by a corresponding change in the thermal conductivity. The results on the phonon lifetime can be interpreted in terms of competition between elastic Bragg scattering and inelastic phonon-phonon scattering. Our results suggest that band effects due to the phononic structure may impact inelastic scattering in addition to elastic scattering.

**Acknowledgments**

The authors gratefully acknowledge support from NSF grant #0924103.

## References

* Electronic address: `deymier@email.arizona.edu`

[1] P. Hyldgaard and G. D. Mahan, in *Thermal Conductivity*, Vol. 23, (Technomic, Lancaster, PA, 1996).
G. Chen, C. L. Tien, X. Wu, and J. S. Smith, J. Heat Transfer **116**, 325 (1994).
W. S. Capinski and H. J. Maris, Physica B **219 & 220**, 699 (1996).
[2] J. O. Vasseur, B. Djafari-Rouhani, L. Dobrzynski, M. S. Kushwaha, and P. Halevi, J. of Physics : Cond. Matter **6**, 8759 (1994).
[3] M. M. Sigalas and E. N. Economou, Solid State Comm. **86**, 141 (1993).
[4] J. O. Vasseur, B. Djafari-Rouhani, L. Dobrzynski, and P. A. Deymier, J. of Physics: Condensed Matter, **9**, 7327 (1997).
[5] For a review, see M. S. Kushwaha, Recent Res. Devel. Applied Phys., **2**, 743 (1999).
[6] M. S. Kushwaha, P. Halevi, L. Dobrzynski, and B. Djafari-Rouhani, Phys. Rev. Lett. **71**, 2022 (1993).
[7] M. S. Kushwaha, Appl. Phys. Let. **70**, 3218 (1997).
[8] J. O. Vasseur, P. A. Deymier, B. Chenni, B. Djafari-Rouhani, L. Dobrzynski and D. Prevost, Phys. Rev. Lett. **86**, 3012 (2001).
J. O. Vasseur, P. A. Deymier, G. Frantziskonis, G. Hong, B. Djafari-Rouhani and L. Dobrzynski, J. of Phys. Condensed matter, **10**, 6051 (1998).
[9] R. E. Vines, J. P. Wolfe, A. V. Every, Phys. Rev. B, **60**, 11871 (1999).
[10] F. R. Montero de Espinosa, E. Jimenez, and M. Torres, Phys. Rev. Lett. **80**, 1208 (1998).
[11] W. M. Robertson and J. F. Rudy III, J. Acoust. Soc. Am. **104**, 694 (1998).
[12] J. V. Sanchez-Pérez, D. Caballero, R. Martinez-Sala, J. Rubio, J. Sanchez-Dehesa, F. Meseguer, J. Llinares and F. Galvez, Phys. Rev. Lett. **80**, 5325 (1998).
D. Caballero, J. Sanchez-Dehesa, J. Rubio, R. Martinez-Sala, J. V. Sanchez-Perez, F. Meseguer

and J. Llinares, Phys. Rev. E **60**, R6316 (1999).
J. O. Vasseur, P. A. Deymier, A. Khelif, Ph. Lambin, B. Djafari-Rouhani, L. Dobrzynski, A. Akjouj, N. Fettouhi and J. Zemmouri, Phys. Rev. E **65**, 056608-1 (2002).
[13] M. Torres, F. R. Montero de Espinosa, D. Garcia Pablos and N. Garcia, Phys. Rev. Lett. **82**, 3054 (1999).
A. Khelif, B. Djafari-Rouhani, J. O. Vasseur and P. A. Deymier, Phys. Rev. B **68**, 024302 (2003).
[14] M. Torres, F. R. Montero de Espinosa, J. L. Aragon, Phys. Rev. Lett. **86**, 4282 (2001).
[15] M. Kafesaki, M. M. Sigalas and N. Garcia, Phys. Rev. Lett. **85**, 4044 (2000) and Physica B **296**, 190 (2001).
[16] A. Khelif, B. Djafari-Rouhani, J. O. Vasseur, P. A. Deymier, Phys. Rev. B **68**, 024302 (2003).
J. O. Vasseur, P. A. Deymier, M. Beaugeois, Y. Pennec, B. Djafari-Rouhani, and D. Prevost, Zeischrift for Krystallography **220**, 829-835 (2005).
Y. Pennec, B. Djafari-Rouhani, J. O. Vasseur, A. Khelif, P. A. Deymier, Phys. Rev. E **69**, 046608 (2004).
A. Khelif, P. A. Deymier, B. Djafari-Rouhani, J. O. Vasseur and L. Dobrzynski, Journal of Appl. Phys. **94**, 1308 (2003).
A. Khelif, B. Djafari-Rouhani, J. O. Vasseur, P. A. Deymier, Ph. Lambin, L. Dobrzynski, Phys. Rev. B. **65**, 174308-1 (2002).
[17] Y. Tanaka and S. Tamura, Phys. Rev. B **58**, 7958 (1998).
[18] Y. Tanaka and S. Tamura, Phys. Rev. B **60**, 13294 (1999).
[19] T. T. Wu, Z. G. Huang, S. Lin, Phys. Rev. B **69**, 094301 (2004).
[20] V. Laude, M. Wilm, S. Benchabane, and A. Khelif, Phys. Rev. E **71**, 036607 (2005).
[21] J. J. Chen, B. Qin, and J. C. Cheng, Chin. Phys. Lett. **22**, 1706 (2005).
[22] J. O. Vasseur, P. A. Deymier, B. Djafari-Rouhani, and Y. Pennec, Phys. Rev. B **77**, 085415 (2008).
[23] B. Manzanares-Martinez and F. Ramos-Mendieta, Phys. Rev. B **65**, 134303 (2003).
[24] R. Sainidou and N. Stefanou, Phys. Rev. B **73**, 184301 (2006).
[25] J. O. Vasseur, A-C. Hladky-Hennion, B. Djafari-Rouhani, F. Duval, B. Dubus, Y. Pennec and P. A. Deymier, J. Appl. Phys. **10**, 114904 (2007).
[26] T. T. Wu, Z. G. Huang, and S. Y. Liu, Z. Kristallogr. **220**, 841 (2005).
T. T. Wu, L. C. Wu, and Z. G. Huang, J. Appl. Phys. **97**, 094916 (2005).
[27] S. Benchabane, A. Khelif, J-Y. Rauch, L. Robert, and V. Laude, Phys. Rev. E **73**, 065601 (2006).
[28] Xinya Zhang, T. Jackson, E. Lafond, P. Deymier and J. Vasseur, Appl. Phys. Lett. **88**, 041911 (2006).
[29] I. E. Psarobas and M. M. Sigalas, Phys. Rev. B **66**, 052302 (2002).
[30] M. M. Sigalas and N. Garcia, J. Appl. Phys. **87**, 3122 (2000).
[31] Suxia Yang, J. H. Page, Zhengyou Liu, M. L. Cowan, C. T. Chan, and Ping Sheng, Phys. Rev. Lett. **88**, 104301 (2002).
[32] R. Sainidou, N. Stefanou and A. Modinos, Phys. Rev. B **66**, 212301 (2002).
[33] I. E. Psarobas, N. Stefanou and A. Modinos, Phys. Rev. B **62**, 278 (2000).
[34] Zhengyou Liu, Xixiang Zhang, Yiwei Mao, Y. Y. Zhu, Zhiyu Yang, C. T. Chan, and Ping Sheng, Science **289**, 1734 (2000).
[35] Zhengyou Liu, C. T. Chan and Ping Sheng, Phys. Rev. B **65**, 165116 (2002).
[36] Zhengyou Liu, C. T. Chan and Ping Sheng, A. L. Goertzen, and J. H. Page, Phys. Rev. B **62**, 2446 (2000).
[37] I. E. Psarobas, N. Stefanou, and A. Modinos, Phys. Rev. B **62**, 5536 (2000).

[38] Haripin Chandra, P. A. Deymier and J. O. Vasseur, Phys. Rev. B **70**, 054302 (2004).
[39] J. Li, K. H. Fung, Z. Y. Liu, P. Sheng, and C. T. Chan, in *Physics of Negative Refraction and Negative Index Materials*, Springer Series in Materials Science, Vol. 98 , (Springer Berlin Heidelberg 2007) Chap. 8.
N. Fang, D. Xi, J. Xu, M. Ambati, W. Srituravanich, C. Sun, X. Zhang, Nature Mater. **5**, (2006).
[40] S. Yang, J. H. Page, Z. Liu, M. L. Cowan, C. T. Chan and P. Sheng, Phys. Rev. Lett. **93**, 024301 (2004).
[41] J. H. Page, A. Sukhovich, S. Yang, M. L. Cowan, F. Van der Biest, A. Tourin, M. Fink, Z. Liu, C. T. Chan, and P. Sheng, Phys. Stat. Sol. (b) **241**, 3454 (2004).
[42] K. Imamura and S. Tamura, Phys. Rev. B **70**, 174308 (2004).
X. Zhang and Z. Liu, Appl. Phys. Lett. **85**, 341 (2004).
[43] M. Ke, Z. Liu, Z. Cheng, J. Li, P. Peng, and J. Shi, Solid State Comm. **142**, 177 (2007).
[44] A. Sukhovich, L. Jing, and J. Page, Phys. Rev. B **77**, 014301 (2008).
[45] M. Ambati, N. Fang, C. Sun, and X. Zhang, Phys. Rev. B **75**, 195447 (2007).
[46] A. Sukhovich, B. Merheb, K. Muralidharan, J. O. Vasseur, Y. Pennec, P. A. Deymier and J. Page, Phys. Rev. lett. **102**, 154301 (2009).
[47] J. Bucay, E. Roubssel, J. O. Vasseur, P. A. Deymier, A.-C. Hladky-Hennion, Y. Pennec, K. Muralidharan, B. Djafari-Rouhani and B. Dubus, Phys. Rev. B **79**, 214305 (2009).
[48] T. Gorishnyy, C. K. Ullal, M. Maldovan, G. Fytas and E. L. Thomas, Phys. Rev. Lett. **94**, 115501 (2005).
[49] J.-N. Gillet, Y. Chalopin, and S. Volz, J. Heat Transfer, **131**, 043206 (2009).
[50] G. P. Srivastava, *The Physics of Phonons*, (Adam Hilger, Bristol, 1990).
[51] J. Tersoff, Phys. Rev. B, **39**, 5566 (1989).
[52] A. J. H. McGaughey and M. Kaviani, Advances in Heat Transfer, **39**, 169 (2006).
[53] J. Che, T. Cagin and W. A. Goddard III, J. Chem. Phys. **113**, 6888 (2000).
[54] General Utility Lattice Program, `https://www.ivec.org/gulp/`
[55] Turney *et al.*, Phys. Rev. B **79**, 064301 (2009).